Electron acceleration in a secondary magnetic island formed during magnetic reconnection with a guide field

Huanyu Wang, Quanming Lu, Can Huang, and Shui Wang

Citation: Physics of Plasmas **24**, 052113 (2017); doi: 10.1063/1.4982813
View online: http://dx.doi.org/10.1063/1.4982813
View Table of Contents: http://aip.scitation.org/toc/php/24/5
Published by the American Institute of Physics

PHYSICS OF PLASMAS 24, 052113 (2017)

Electron acceleration in a secondary magnetic island formed during magnetic reconnection with a guide field

Huanyu Wang,[1,2] Quanming Lu,[1,2,a)] Can Huang,[1,2] and Shui Wang[1,2]
[1]*CAS Key Laboratory of Geospace Environment, Department of Geophysics and Planetary Science, University of Science and Technology of China, Hefei 230026, China*
[2]*Collaborative Innovation Center of Astronautical Science and Technology, Hefei 230026, China*

(Received 24 January 2017; accepted 19 April 2017; published online 3 May 2017)

Secondary magnetic islands may be generated in the vicinity of an X line during magnetic reconnection. In this paper, by performing two-dimensional (2-D) particle-in-cell simulations, we investigate the role of a secondary magnetic island in electron acceleration during magnetic reconnection with a guide field. The electron motions are found to be adiabatic, and we analyze the contributions of the parallel electric field and Fermi and betatron mechanisms to electron acceleration in the secondary island during the evolution of magnetic reconnection. When the secondary island is formed, electrons are accelerated by the parallel electric field due to the existence of the reconnection electric field in the electron current sheet. Electrons can be accelerated by both the parallel electric field and Fermi mechanism when the secondary island begins to merge with the primary magnetic island, which is formed simultaneously with the appearance of X lines. With the increase in the guide field, the contributions of the Fermi mechanism to electron acceleration become less and less important. When the guide field is sufficiently large, the contribution of the Fermi mechanism is almost negligible. *Published by AIP Publishing.* [http://dx.doi.org/10.1063/1.4982813]

I. INTRODUCTION

Magnetic reconnection is a fundamental physical process in a plasma, which is closely related to rapid energy conversion, where magnetic free energy stored in a current sheet is suddenly released, and the plasma is then accelerated and heated.[1–6] Electrons accelerated during magnetic reconnection are thought to provide the non-thermal part of electron spectra observed in many explosive phenomena in space and laboratory plasmas, such as solar flares,[7–9] substorms in Earth's magnetosphere,[10–12] and disruptions in laboratory fusion experiments.[13,14]

Electrons are found to be accelerated in several sites of magnetic reconnection. They can be accelerated in the vicinity of the X line and pileup region by the reconnection electric field[15–20] and in the jet front where electron motions are adiabatic and electrons are accelerated by Fermi and betatron mechanisms.[21–24] The efficiency of electron acceleration may be enhanced due to the existence of the parallel electric field in the separatrix region to trap these electrons.[25,26] With *in situ* observations in Earth's magnetotail, Wu *et al.*[27] demonstrated that a multistage acceleration in magnetic reconnection is necessary to energize electrons to higher energy. Recently, magnetic islands are found to play an essential role in electron acceleration,[18,28–32] where electrons gain energy when they are reflected from the ends of the contracting magnetic islands.[18,28] Magnetic islands may be formed between two X lines during multiple X line reconnection, which are called as primary magnetic islands, or in an extended electron diffusion region, which are named as secondary islands.[5,33–35] Electrons are also highly energized during the coalescence of magnetic islands,[31,36–39] while the coalescence of magnetic islands during magnetic reconnection has been *in situ* observed in Earth's magnetotail with Cluster spacecraft.[40,41]

With a guide-center theory, Wang *et al.*[39] analyzed the mechanisms of electron acceleration during the coalescence of magnetic islands, and the islands are formed in multiple X line magnetic reconnection with a guide field. Here, due to the existence of the strong guide field, electron motions can be considered to be adiabatic, and a guide-center approximation can be used to analyze electron motions in the guide field reconnection. Under the guiding-center approximation, the evolution of the energy ε of a single electron can be given as[42,43]

$$\frac{d\varepsilon}{dt} = (\mu/\gamma)\partial_t B - e\left(v_{||}\boldsymbol{b} + \boldsymbol{v}_c + \boldsymbol{v}_g\right)\cdot\boldsymbol{E}, \qquad (1)$$

where $\boldsymbol{b} = \boldsymbol{B}/|\boldsymbol{B}|$, $\mu = m_e\gamma^2 v_\perp^2/2B$ is the magnetic moment, γ is the Lorentz factor, and $v_{||} = \boldsymbol{v}\cdot\boldsymbol{b}$. $\boldsymbol{v}_c = (v_{||}^2\boldsymbol{b}/\Omega_{ce})\times\boldsymbol{\kappa}$ and $\boldsymbol{v}_g = (v_\perp^2\boldsymbol{b}/(2\Omega_{ce}))\times(\nabla B/B)$ are the curvature and gradient B drifts, respectively. $\Omega_{ce} = eB/\gamma m_e c$ is the electron cyclotron frequency, and $\boldsymbol{\kappa} = \boldsymbol{b}\cdot\nabla\boldsymbol{b}$ is the curvature. Eq. (1) can be described as follows after summing all particles in a local region:[43]

$$\frac{dU}{dt} = E_{||}J_{||} + \frac{p_\perp}{B}\left(\frac{\partial B}{\partial t} + \boldsymbol{u}_E\cdot\nabla B\right) + \left(p_{||} + m_e n u_{||}^2\right)\boldsymbol{u}_E\cdot\boldsymbol{\kappa}, \qquad (2)$$

where U is the kinetic energy, $\boldsymbol{u}_E$ is the '$\boldsymbol{E}\times\boldsymbol{B}$' drift velocity, and $u_{||}$ is the bulk velocity parallel to the magnetic field. n is the electron density and $p_\perp$ and $p_{||}$ are the perpendicular and parallel pressures, respectively. The first term in Eq. (2) is the acceleration by the parallel electric field, and the

a)Author to whom correspondence should be addressed. Electronic mail: qmlu@ustc.edu.cn

second term is the betatron mechanism corresponding to perpendicular heating or cooling due to the conservation of magnetic moment μ. The last term drives parallel acceleration, which arises from the first-order Fermi mechanism.[42,43] Wang *et al.*[39] found that electrons are mainly accelerated by the parallel electric field and Fermi mechanism during the formation and coalescence of magnetic islands in multiple X line reconnection, and with the increase in the guide field, the contributions of Fermi acceleration become less and less important. Satellite observations have evidenced that electrons can also be accelerated in a secondary island.[34] In this paper, with a guide-center theory, we quantitatively analyze the mechanisms of electron acceleration during the formation of a secondary island in an extended electron diffusion region and its coalescence with a primary island.

This paper is organized as follows: In Section II, we delineate our simulation model. The simulation results are presented in Section III. We summarize our results and give discussion in Section IV.

II. SIMULATION MODEL

A two-dimensional (2D) particle-in-cell (PIC) simulation model is used in this paper to investigate the mechanisms of electron acceleration during the evolution of a secondary island formed in magnetic reconnection with a guide field. In our PIC simulations, the electromagnetic fields are defined on the grids and updated by solving the Maxwell equations with a full explicit algorithm, and ions and electrons are advanced in these electromagnetic fields. The initial configuration of the magnetic field consists of a uniform guide field superimposed by a Harris equilibrium. The magnetic field and the corresponding number density are given by

$$\boldsymbol{B}_0(z) = B_0 \tanh(z/\delta)\boldsymbol{e}_x + B_{y0}\boldsymbol{e}_y, \tag{3}$$

$$n(z) = n_b + n_0 \mathrm{sech}^2(z/\delta), \tag{4}$$

where B_0 is the asymptotic magnetic field, δ is the half-width of the current sheet, B_{y0} is the initial guide field perpendicular to the reconnection plane, n_b is the number density of the background plasma, and n_0 is the peak Harris number density. The initial distribution functions for ions and electrons are Maxwellian with a drift speed in the y direction, and the drift speeds satisfy the following equation: $V_{i0}/V_{e0} = -T_{i0}/T_{e0}$, where $V_{e0}(V_{i0})$ and $T_{e0}(T_{i0})$ are the initial drift speed and the temperature of electrons (ions), respectively. We set $T_{i0}/T_{e0} = 4$ and $n_b = 0.2n_0$ in our simulations. The initial half-width of the current sheet is set to be $\delta = 0.5d_i$ (where $d_i = c/\omega_{pi}$ is the ion inertial length defined on n_0) and the mass ratio $m_i/m_e = 100$. The light speed is $c = 15v_A$, where v_A is the Alfven speed based on B_0 and n_0.

The computations are carried out in a rectangular domain in the (x, z) plane with the dimension $L_x \times L_z = (51.2d_i) \times (12.8d_i)$. The grid number is $N_x \times N_z = 1024 \times 256$. Therefore, the spatial resolution is $\Delta x = \Delta z = 0.05d_i$, and the time step is $\Omega_i t = 0.001$, where $\Omega_i = eB_0/m_i$ is the ion gyro-frequency. We employ more than 5×10^7 particles per species to simulate the plasma. The periodic boundary conditions are used along the x axis, and the ideal conducting boundary conditions for the electromagnetic field and reflected boundary condition for particles are used in the z direction. The reconnection is initiated by a small flux perturbation, which bypasses the linear growth rate of the tearing mode. The perturbation has the form $\delta\psi = \psi_0 \cos[\pi(z - L_z/2)/L_z] \cdot \{\cosh^{-2}[(x - L_x/2)/k_x] + \cosh^{-2}(x/k_x)\}$. Here, the initial disturbance amplitude ψ_0 is set to be $0.05B_0 d_i$.

In this paper, we run three cases with the initial guide field $B_{y0} = 0.5B_0$, 1.0B$_0$, and $2.0B_0$ where electron motions are almost kept as adiabatic, and the guide-center approximation can be used to investigate the mechanisms to produce the non-thermal electrons during the evolution of the secondary island in magnetic reconnection.

III. SIMULATION RESULTS

We first analyze the reconnection case with the initial guide field $B_{y0} = 1.0B_0$, and reconnection begins at about $\Omega_i t = 15$. Figure 1 shows the distribution of high energy electrons n'_e/n_e at $\Omega_i t = 28$, 30, 32, 34, and 36 for the case with the initial guide field $B_{y0} = 1.0B_0$, where n'_e is the number density of electrons with energy $\varepsilon > 0.1m_e c^2$ and n_e is the total electron number density. The magnetic field lines are also plotted in the figure for reference. At first, two X lines are formed in the current sheet due to the multiple X line reconnection, and two primary magnetic islands (around $x = 13c/\omega_{pi}$ and $38c/\omega_{pi}$, respectively) are generated in the simulation domain. High energy electrons are distributed in the vicinity of the reconnection sites and at the edge of the primary islands. Then, at about $\Omega_i t = 32$, a secondary island

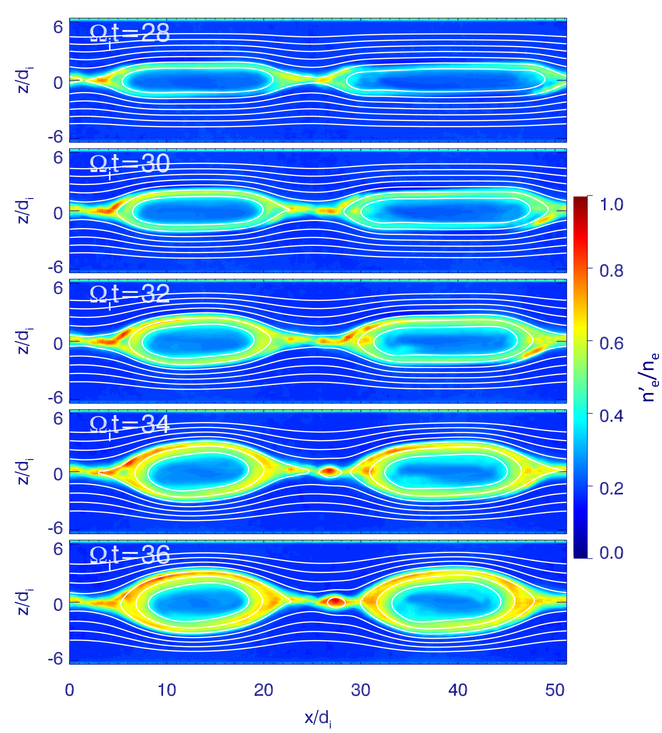

FIG. 1. The distribution of high energy electrons n'_e/n_e at $\Omega_i t = 28$, 30, 32, 34, and 36 for the case with the initial guide field $1.0B_0$ (from the top to the bottom), where n'_e is the number density of electrons with energy $\varepsilon > 0.1m_e c^2$ and n_e is the total electron number density. The magnetic field lines are also plotted in the figure for reference.

is generated in the extended electron diffusion region around $x = 25.6d_i$. At last, the secondary island is merged with the primary island around $x = 38c/\omega_{pi}$. We can also find that the high energy electrons are enhanced in the secondary island, which means that electrons can be accelerated in the secondary island.

Figure 2 presents the contributions of the parallel electric field and Fermi and betatron mechanisms to electron acceleration during magnetic reconnection at $\Omega_i t = 28$, 30, 32, 34, and 36 for the case with the initial guide field $B_{y0} = 1.0B_0$, and contributions are calculated based on Eq. (2). Electrons are accelerated mainly by the parallel electric field and Fermi mechanism. The electron acceleration by the parallel electric field occurs in the vicinity of the X line (includes the secondary island) due to the existence of the reconnection electric field, while electrons can be accelerated by the Fermi mechanism when they are trapped in both the primary magnetic islands and secondary island. How electrons are accelerated in the primary islands has been already thoroughly studied in the previous work.[39] In this paper, we will demonstrate how the formation of a secondary island in the vicinity of the X line influences electron acceleration in magnetic reconnection.

In order to evaluate different mechanisms of electron acceleration in the secondary island, we trace a defined flux tube whose outer boundary has the magnetic flux $\psi = 1.7B_0d_i$ in the secondary island and then integrate the contributions from the acceleration mechanisms based on Eq. (2): the parallel electric field, Fermi mechanism, and betatron mechanism over the flux tube. Figure 3(a) shows the closed magnetic field line with the magnetic flux $\psi = 1.7B_0d_i$ marked with the red solid line at $\Omega_i t = 33.5$ for the case with the initial guide field $B_{y0} = 1.0B_0$. During the period from $\Omega_i t = 33.2$ to $\Omega_i t = 37$, the magnetic field line (with the magnetic flux $\psi = 1.7\,B_0d_i$) formed a closed configuration. The core region of the secondary island was circled by it. At $\Omega_i t = 33.2$, the flux tube circled by the field line with $\psi = 1.7B_0d_i$ just begins to be generated, and at $\Omega_i t = 37.3$, the same flux tube begins to merge with the primary island in the right side of the simulation domain. Figure 3(b) exhibits the time evolution of the contributions from the parallel electric field (cyan) and Fermi (red) and betatron (blue) mechanisms to the enhancement of energetic electrons in the flux tube for the case with the initial guide field $B_{y0} = 1.0B_0$. The parallel electric field works during the periods when the flux tube begins to be formed and merge with the primary island. However, the Fermi mechanism only works when the flux tube begins to merge with the primary. The contribution of the betatron mechanism to energetic electrons is negligible. Figure 3(c) shows the measurement of the acceleration term dU_e/dt, which is calculated from the particles located in the flux tube at $\Omega_i t = 33.2$, and the sum of the contributions from the parallel electric field and Fermi and betatron mechanisms based on Eq. (2). The measurement of the acceleration term dU_e/dt is consistent with the sum of the contributions from the parallel electric field and Fermi and betatron mechanisms. It means that the adiabatic theory used in this paper works well to study electron acceleration.

Figure 4 shows the evolution of the secondary island at $\Omega_i t = 31$, 33, 35, 37, and 38 for the case with the initial guide field $B_{y0} = 1.0B_0$, and different colors denote different layers in the secondary island. Around $\Omega_i t = 33$, the secondary island is formed, and then it moves toward the right until merges with the primary island. Figures 5(a)–5(d) plot the contributions of the parallel electric field and Fermi and betatron mechanisms in different layers of the secondary

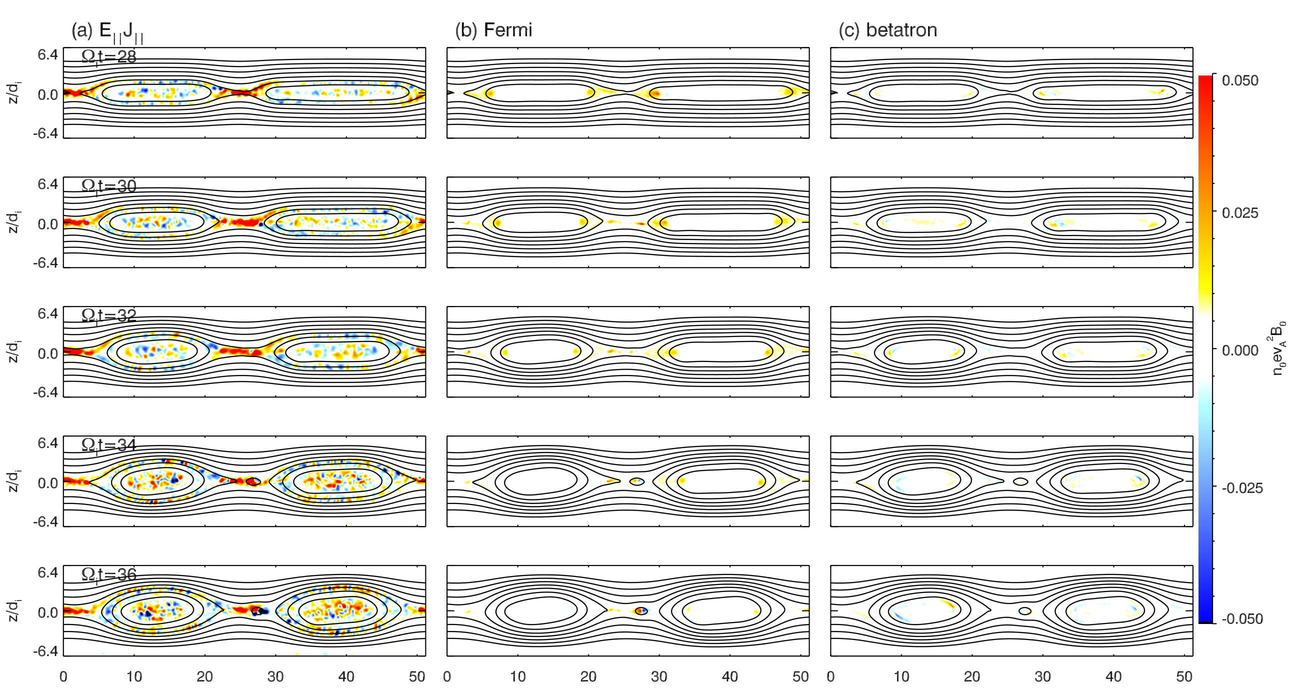

FIG. 2. The contributions of the parallel electric field and Fermi and betatron mechanisms to electron acceleration during magnetic reconnection at $\Omega_i t = 28$, 30, 32, 34, and 36 for the case with the initial guide field $1.0B_0$ (from the top to the bottom), and contributions are calculated based on Eq. (2).

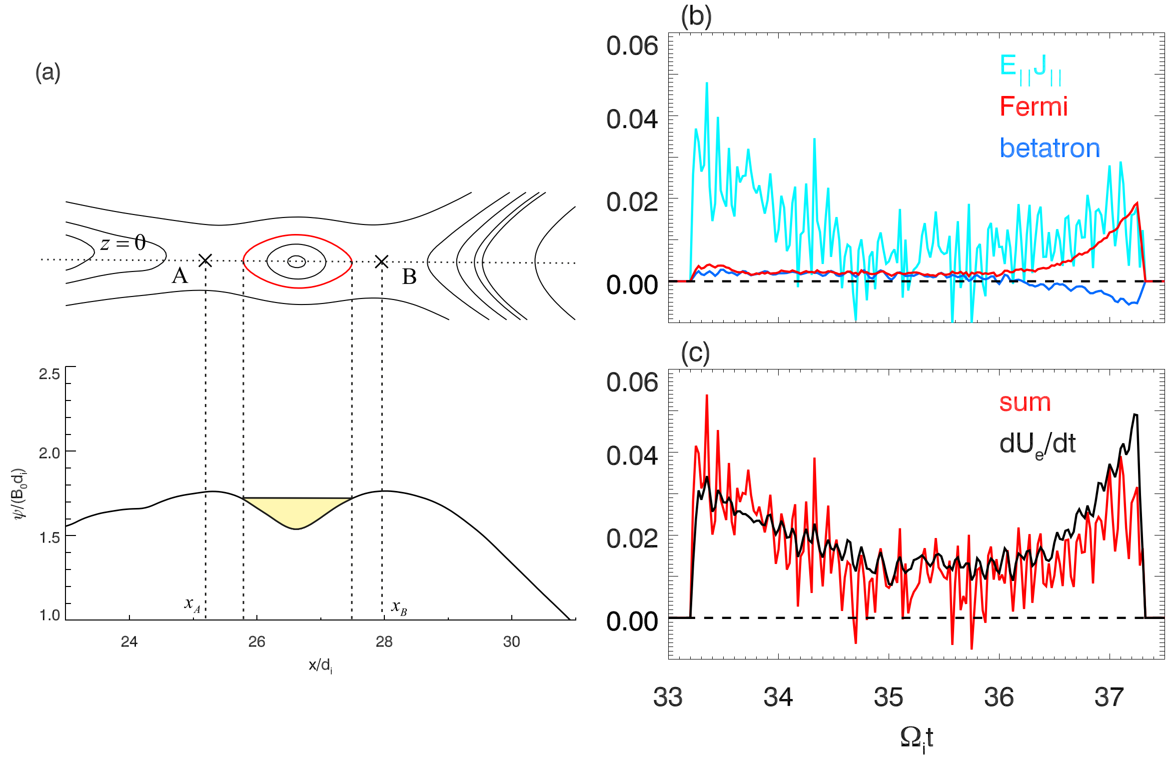

FIG. 3. (a) The magnetic field lines and magnetic flux ψ associated with the secondary island for the case with the initial guide field $1.0B_0$, and the red line denotes the closed magnetic field line with the magnetic flux $\psi = 1.7B_0 d_i$ marked with the red solid line at $\Omega_i t = 33.5$. (b) The time evolution of the contributions from the parallel electric field (cyan) and Fermi (red) and betatron (blue) mechanisms to the enhancement of energetic electrons in the flux tube. (c) The measurement of the acceleration term dU_e/dt, which is calculated from the particles located in the flux tube from $\Omega_i t = 33.2$ to $\Omega_i t = 37.3$, and the sum of the contributions from the parallel electric field and Fermi and betatron mechanisms based on Eq. (2).

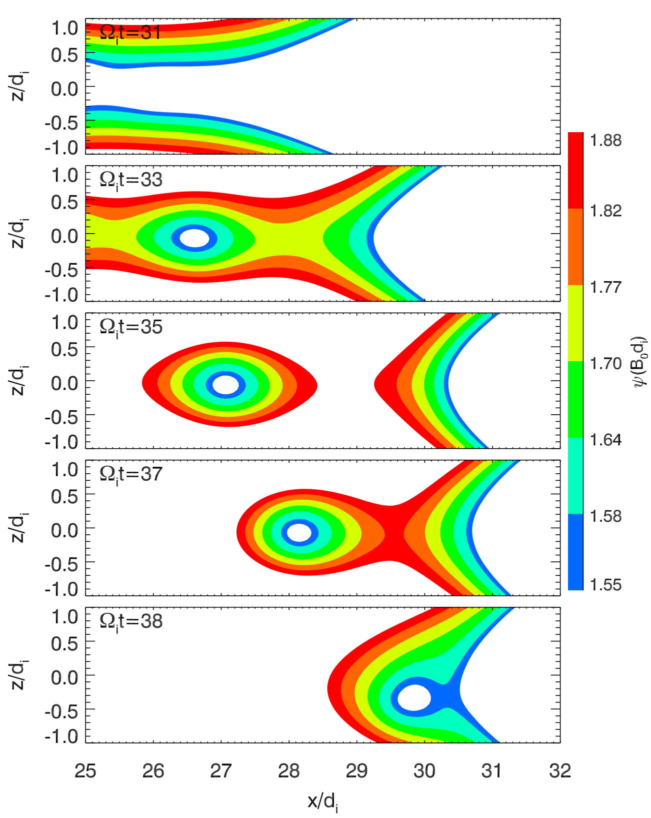

FIG. 4. The evolution of the secondary island at $\Omega_i t = 31$, 33, 35, 37, and 38 for the case with the initial guide field $1.0B_0$ and different colors denote different layers in the secondary island.

island for the case with the initial guide field $B_{y0} = 1.0B_0$, and different layers denote different colors corresponding to those in Fig. 4. Similar to that in Fig. 3, electrons are accelerated by the Fermi mechanism only when the secondary island begins to merge with the primary island, while electrons can be accelerated by the parallel electric field when the secondary island is formed and merges with the primary island. We further find that the contributions of both the parallel electric field and Fermi mechanisms are larger in the inner layers than those in the outer layers.

This is illustrated more clearly in Fig. 6, in which the spatial distributions of the electron nongyrotropy, the contributions of the parallel electric field, and Fermi and betaron mechanisms to energetic electrons in the secondary island at $\Omega_i t =$ (a)33 and (b)37 for the case with the initial guide field $B_{y0} = 1.0B_0$ are shown. The electron nongyrotropy is calculated by $D_{ng} = \frac{2\sqrt{\Sigma_{i,j}N_{ij}^2}}{Tr(\mathbf{P}_e)}$, where $\mathbf{P}_e$ is the electron full pressure tensor and N_{ij} represents the matrix elements of $\mathbf{N}$, defined as the nongyrotropic part of the electron full pressure tensor.[44] The electron nongyrotropy is almost zero in the secondary island, and it means that the guide-center theory can be used to analyze the electron acceleration here. The times $\Omega_i t = 33$ and 37 stand for the periods, when the secondary island is formed and merges with the primary island, respectively. When the secondary island is formed, the contribution of the parallel electric field exists inside the secondary island due to the existence of the reconnection electric field in the vicinity of the X line. However, when the secondary island begins

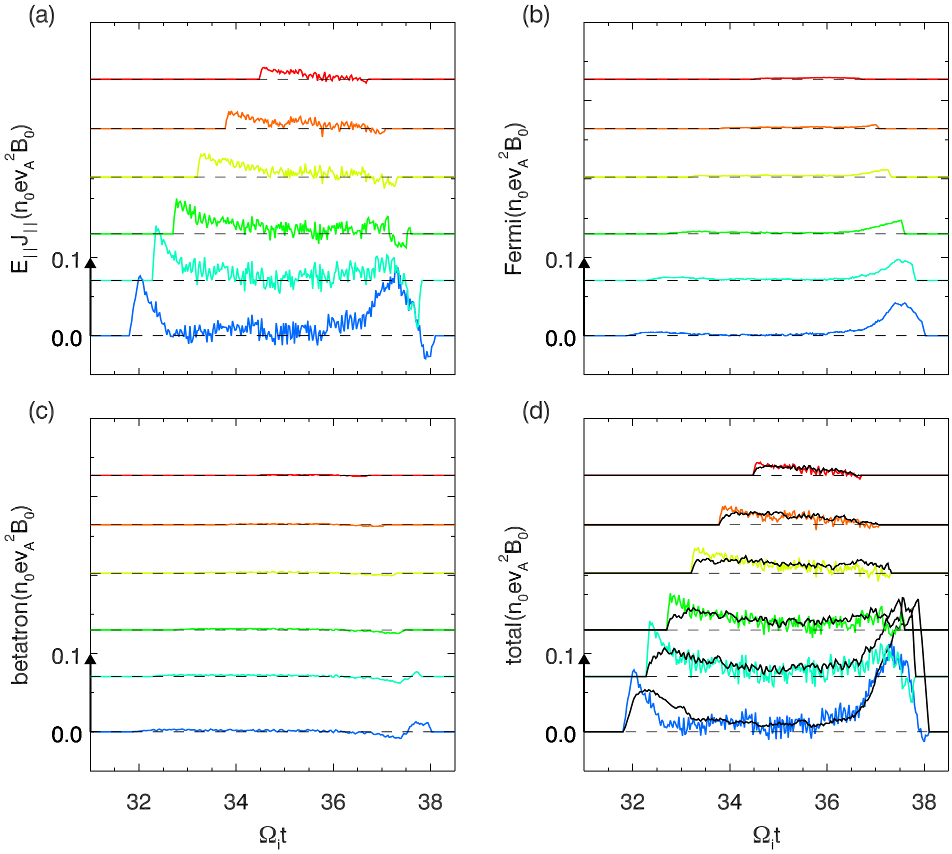

FIG. 5. The contributions from (a) the parallel electric field and (b) Fermi and (c) betatron mechanisms to electron acceleration in different layers of the secondary island for the case with the initial guide field $1.0B_0$, while (d) shows the sum of these contributions. Different layers denote different colors corresponding to those in Fig. 4. Also in (d), the black lines plot the measurement of the acceleration term dU_e/dt, which is calculated from the particles located in the corresponding layers when the layers are just formed.

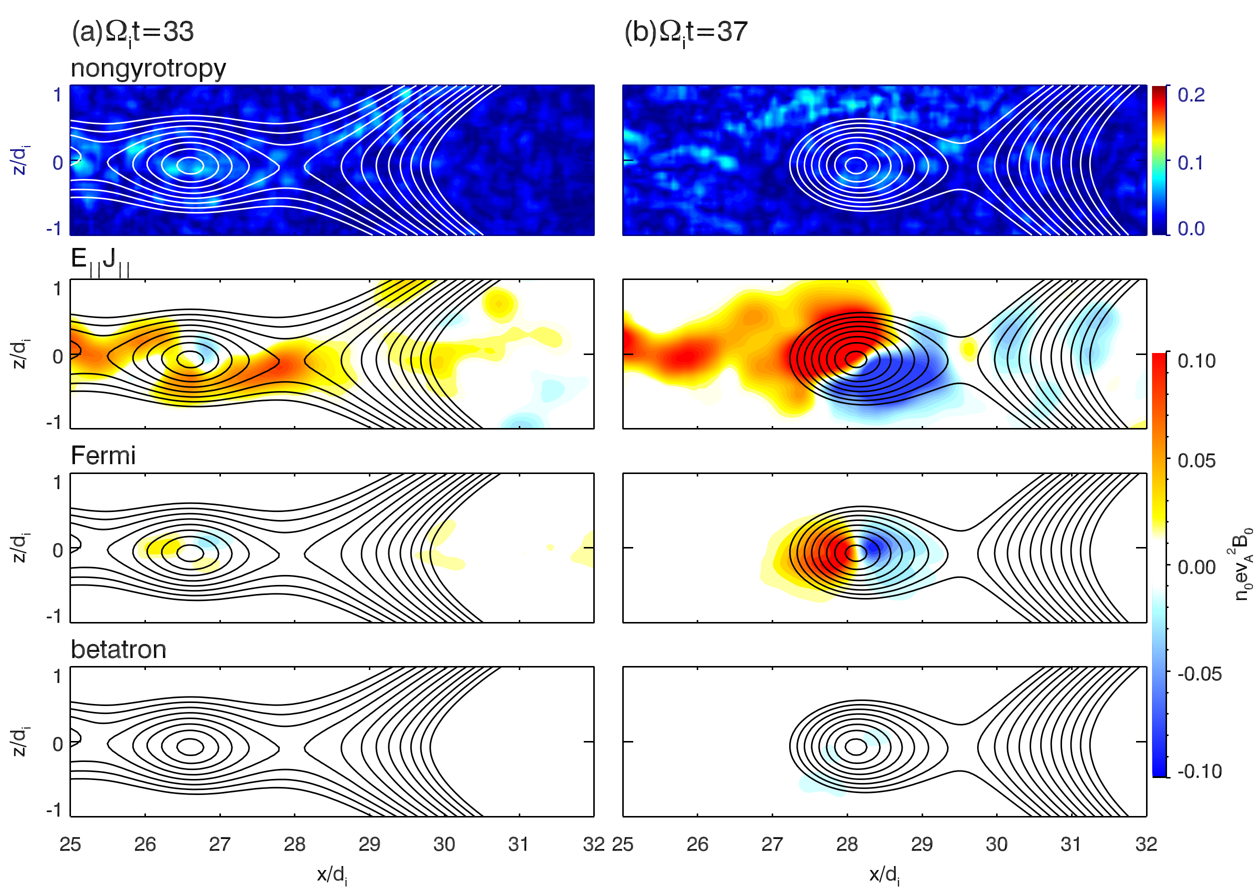

FIG. 6. The spatial distributions of the electron nongyrotropy, the contributions of the parallel electric field, and Fermi and betaron mechanisms to energetic electrons in the secondary island at $\Omega_i t$ =(a) 33 and (b) 37 for the case with the initial guide field $1.0B_0$.

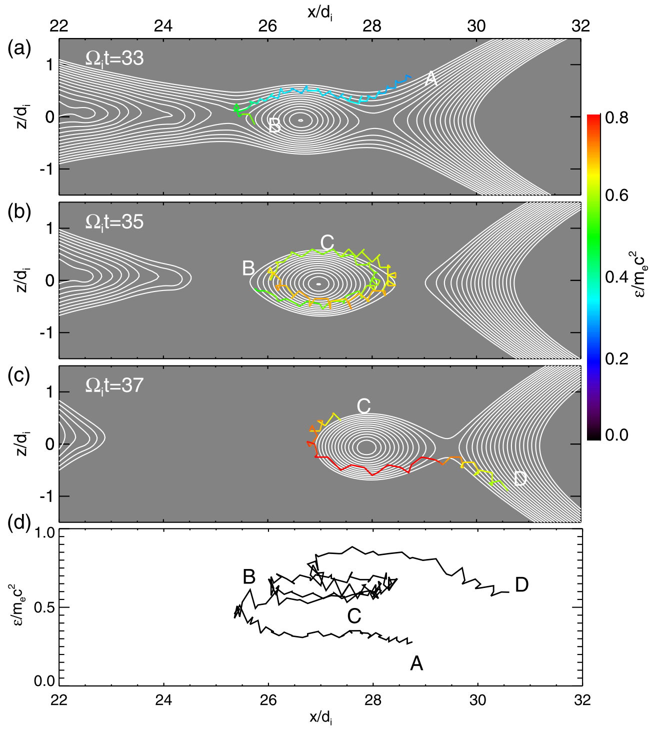

FIG. 7. ((a)–(c)) The trajectories of a typical electron during (a) $32.5 < \Omega_i t < 34$, (b) $34 < \Omega_i t < 36.25$, and (c) $36.25 < \Omega_i t < 37.4$ for the case with the initial guide field $1.0B_0$. The color of the trajectory indicates the kinetic energy of the electron. The magnetic field line is plotted at (a) $\Omega_i t = 33$, (b) $\Omega_i t = 35$, and (c) $\Omega_i t = 37$, respectively. (d) The whole trajectory is shown in a format of electron kinetic energy $\varepsilon/m_e c^2$ versus the spatial location x.

to merge with the primary island, the contribution of Fermi mechanisms forms a bipolar distribution in the secondary island. The positive term in the left part is stronger than the negative term in the right part. The net effect of the Fermi mechanism in the secondary island is positive for electron acceleration, which is shown in Fig. 5(b). Simultaneously, the reconnection electric field with the direction reverse to that in the vicinity of the X line is generated around the merging region; therefore, the contributions of the parallel electric field are negative in the right part of the secondary island.

Figures 7(a)–7(c) show the trajectory of a typical electron trapped by the secondary island during different time intervals for the case with the initial guide field $B_{y0} = 1.0B_0$, and Figure 7(d) shows this electron kinetic energy $\varepsilon/m_e c^2$ versus its spatial location x. During the period $32.5 < \Omega_i t < 34$, the secondary island has just been formed, and the electron is trapped and accelerated mainly by the parallel electric field in the secondary island, which has been depicted in Fig. 5. During the period $34 < \Omega_i t < 36.25$, the secondary island moves quickly toward the primary island, and the electron is still trapped in the secondary island and accelerated by the parallel electric field. During the time period $36.25 < \Omega_i t < 37.4$, the secondary island begins to merge with the primary island, and the electron pass through the merging region between the secondary and primary islands. The electron energy increases when it passes through the left end of the secondary island and slightly decreases when it passes through the merging region.

Figure 8(a) shows the spatial distribution of the contributions from the parallel electric field and Fermi and betatron mechanisms to energetic electrons in the secondary island and (b) the time evolution of the contributions from the parallel electric field (green) and Fermi (red) and betatron (blue) mechanisms to the enhancement of energetic electrons in the flux tube (denoted by the green line in Fig. 8(a)) for the case with the initial guide field $B_{y0} = 0.5B_0$. Similar to the results from the case with the initial guide

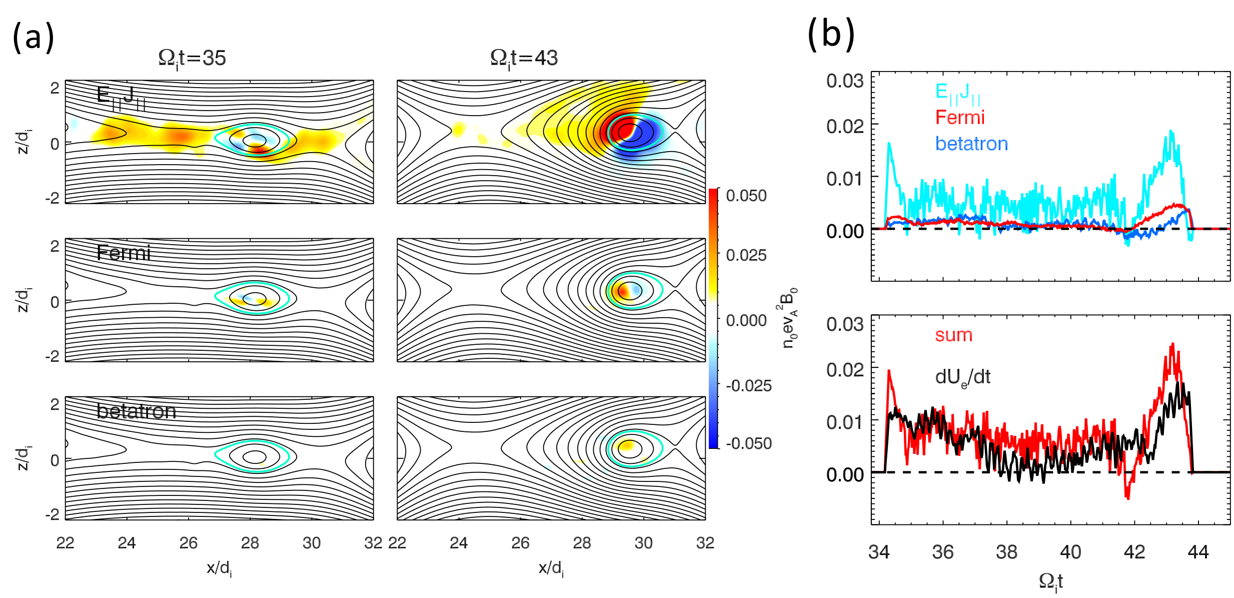

FIG. 8. Results from a simulation with the initial guide field $0.5B_0$. (a) The spatial distributions of power terms: the parallel electric field and Fermi and betatron mechanisms at $\Omega_i t = 36$ and 43. (b) The upper panel shows the time evolution of the contributions from the parallel electric field (green) and Fermi (red) and betatron (blue) the mechanisms to the enhancement of energetic electrons in the flux tube with the boundary $\psi = 4.1B_0 d_i$ (denoted by the green line in (a)). The bottom panel shows the measurement of the acceleration term dU_e/dt, which is calculated from the particles located in the flux tube with the boundary $\psi = 4.1B_0 d_i$, and the sum of the contributions from the parallel electric field and Fermi and betatron mechanisms based on Eq. (2).

field $1.0B_0$, during the formation of the secondary island, the dominated mechanism for electron acceleration is the parallel electric field acceleration. When the secondary island begins to merge with the primary island, the contributions of both the parallel electric field and Fermi mechanism form a bipolar distribution in the secondary island, and their net effects are positive. In this case, the contribution of the betatron mechanism to electron acceleration cannot be neglected because the secondary island can be slightly compressed.

Figure 9(a) shows the spatial distribution of the contributions from the parallel electric field and Fermi and betatron mechanisms to energetic electrons in the secondary island and (b) the time evolution of the contributions from the parallel electric field (green) and Fermi (red) and betatron (blue) mechanisms to the enhancement of energetic electrons in the flux tube (denoted by the green line in Fig. 9(a)) for the case with the initial guide field $B_{y0} = 2.0B_0$. We can find that in this case, only the parallel electric field has contribution to electron acceleration in the secondary island.

IV. CONCLUSIONS AND DISCUSSION

In this paper, with a 2D PIC simulation model, we have studied electron acceleration in a secondary magnetic island generated in a guide field reconnection. A secondary island can be formed in the elongated electron current sheet, and then it moves toward the primary magnetic island until merges with the primary island completely. The parallel electric field and Fermi mechanism are found to play important roles in electron acceleration in the secondary island. During the formation of the secondary island, electrons are mainly accelerated by the parallel electric field due to the existence of the reconnection electric field in the vicinity of the X line. When the secondary island begins to merge with the primary island, electrons can be accelerated by both the parallel electric field and Fermi mechanism. Different from the primary island formed during multiple X line reconnection with a guide field, the secondary island formed in the vicinity of the X line is hard to be compressed, where Fermi acceleration can only work during its merging with the primary island. With the increase in the initial guide field, the formed secondary island becomes more and more difficult to be compressed, which makes the Fermi mechanism less and less important. Compared with electron acceleration in a primary island formed during multiple X line reconnection,[39] the efficiency of electron acceleration in a secondary island formed during an extended electron current is not so high due to its smaller scale size.

In situ observations have evidenced the enhancement of energetic electrons in a secondary island.[12] Drake *et al.*[28] attributed such enhancement of energetic electrons in a secondary island to the Fermi mechanism. However, our simulations show that electrons in a secondary island can be accelerated by both the parallel electric field and Fermi mechanism, and with the increase in the guide field, the contribution from the Fermi mechanism becomes less and less important. When the guide field is sufficiently strong, the contribution from the Fermi mechanism can be neglected. Both simulations[24,33,45,46] and observations[40] have found that plenty of secondary magnetic islands can be generated in an electron current sheet or a large-scale magnetic island. These islands may interact each other,[40] and they should have complicated three-dimensional structures.[45] All these may change the role of secondary islands in electron acceleration during magnetic reconnection, which is our future investigation.

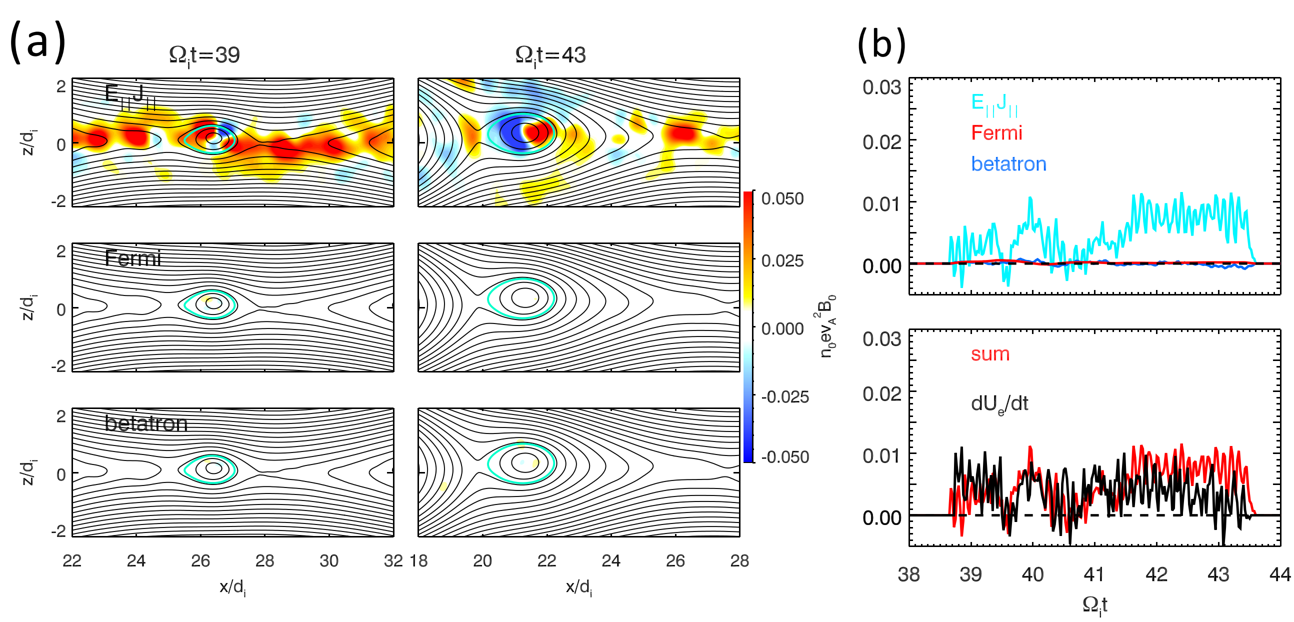

FIG. 9. Results from a simulation with the initial guide field $2.0B_0$. (a) The spatial distributions of power terms: parallel electric field and Fermi and betatron mechanisms at $\Omega_i t = 36$ and 43. (b)The upper panel shows the time evolution of the contributions from the parallel electric field (green) and Fermi (red) and betatron (blue) mechanisms to the enhancement of energetic electrons in the flux tube with the boundary $\psi = 2.2B_0 d_i$ (denoted by the green line in (a)). The bottom panel shows the measurement of the acceleration term dU_e/dt, which is calculated from the particles located in the secondary island with boundary $\psi = 2.2B_0 d_i$, and the sum of the contributions from the parallel electric field and Fermi and betatron mechanisms based on Eq. (2).

ACKNOWLEDGMENTS

This work was supported by the National Science Foundation of China, Grant Nos. 41331067, 41527804, 41474125, 11235009, and 41121003, the Key Research Program of Frontier Sciences, CAS (QYZDJ-SSW-DQC010), and 973 Program (2013CBA01503).

[1]E. N. Parker, J. Geophys. Res. **62**, 509, doi:10.1029/JZ062i004p00509 (1957).
[2]V. M. Vasyliunas, Rev. Geophys. Space Phys. **13**, 303, doi:10.1029/RG013i001p00303 (1975).
[3]D. Biskamp, in *Magnetic Reconnection in Plasmas*, edited by M. G. Haines and K. I. Hopcraft (Cambridge University Press, Cambridge, 2000).
[4]J. Birn, J. F. Drake, M. A. Shay, B. N. Rogers, R. E. Denton, M. Hesse, M. Kuznetsova, Z. Ma, A. Bhattacharjee, A. Otto, and P. L. Pritchett, J. Geophys. Res. **106**, 3715, doi:10.1029/1999JA900449 (2001).
[5]W. Daughton, J. Scudder, and H. Karimabadi, Phys. Plasmas **13**, 072101 (2006).
[6]S. Lu, Q. Lu, C. Huang, and S. Wang, Phys. Plasmas **20**, 061203 (2013).
[7]R. P. Lin and H. S. Hudson, Sol. Phys. **50**, 153 (1976).
[8]J. A. Miller, P. J. Cargill, A. G. Emslie, G. D. Holman, B. R. Dennis, T. N. LaRosa, R. M. Winglee, S. G. Benka, and S. Tsuneta, J. Geophys. Res. **102**, 14631, doi:10.1029/97JA00976 (1997).
[9]R. P. Lin, S. Krucker, G. J. Hurford, D. M. Smith, H. S. Hudson, G. D. Holman, R. A. Schwartz, B. R. Dennis, G. H. Share, and R. J. Murphy, Astrophys. J. Lett. **595**, L69 (2003).
[10]M. Øieroset, R. P. Lin, T. D. Phan, D. E. Larson, and S. D. Bale, Phys. Rev. Lett. **89**, 195001 (2002).
[11]S. Imada, R. Nakamura, P. W. Daly, M. Hoshino, W. Baumjohann, S. Mühlbachler, A. Balogh, and H. Rème, J. Geophys. Res. **112**, A03202, doi:10.1029/2006JA011847 (2007).
[12]R. Wang, Q. Lu, A. Du, and S. Wang, Phys. Rev. Lett. **104**, 175003 (2010).
[13]J. Wesson, *Tokamaks* (Oxford University Press, New York, 1997).
[14]P. V. Savrukhin, Phys. Rev. Lett. **86**, 3036 (2001).
[15]M. Hoshino, T. Mukai, T. Terasawa, and I. Shinohara, J. Geophys. Res. **106**, 25979, doi:10.1029/2001JA900052 (2001).
[16]J. F. Drake, M. A. Shay, W. Thongthai, and M. Swisdak, Phys. Rev. Lett. **94**, 095001 (2005).
[17]P. L. Pritchett, J. Geophys. Res. **111**, A10212, doi:10.1029/2006JA011793 (2006).
[18]X. Fu, Q. Lu, and S. Wang, Phys. Plasmas **13**, 012309 (2006).
[19]C. Huang., Q. Lu, and S. Wang, Phys. Plasmas **17**, 072306 (2010).
[20]J. Egedal, A. Le, and W. Daughton, Phys. Plasmas **20**, 061201 (2013).
[21]H. Fu, Y. V. Khotyaintsev, M. André, and A. Vaivads, Geophys. Res. Lett. **38**, L16104, doi:10.1029/2011GL048528 (2011).
[22]M. Wu, Q. Lu, M. Volwerk, Z. Vörös, T. Zhang, L. Shan, and C. Huang, J. Geophys. Res. **118**, 4804, doi:10.1002/jgra.50456 (2013).
[23]J. Birn, M. Hesse, R. Nakamura, and S. Zaharia, J. Geophys. Res. **118**, 1960, doi:10.1002/jgra.50132 (2013).
[24]C. Huang, Q. Lu, F. Guo, M. Wu, A. Du, and S. Wang, Geophys. Res. Lett. **42**, 7282, doi:10.1002/2015GL065690 (2015).
[25]J. Egedal, W. Daughton, and A. Le, Nat. Phys. **8**, 321 (2012).
[26]R. Wang, Q. Lu, Y. V. Khotyaintsev, M. Volwerk, A. Du, R. Nakamura, W. D. Gonzalez, X. Sun, W. Baumjohann, X. Li, T. Zhang, A. N. Fazakerley, C. Huang, and M. Wu, Geophys. Res. Lett. **41**, 4851, doi:10.1002/2014GL061157 (2014).
[27]M. Wu, C. Huang, Q. Lu, M. Volwerk, R. Nakamura, Z. Vörös, T. Zhang, and S. Wang, J. Geophys. Res. **120**, 6320, doi:10.1002/2015JA021165 (2015).
[28]J. F. Drake, M. Swisdak, H. Che, and M. A. Shay, Nature **443**, 553 (2006).
[29]P. L. Pritchett, Phys. Plasmas **15**, 102105 (2008).
[30]L. J. Chen, A. Bhattacharjee, P. A. Puhl-Quinn, H. Yang, N. Bessho, S. Imada, S. Mühlbachler, P. W. Daly, B. Lefebvre, Y. Khotyaintsev, A. Vaivads, A. Fazakerley, and E. Georgescu, Nat. Phys. **4**, 19 (2008).
[31]M. Oka, T. D. Phan, S. Krucker, M. Fujimoto, and I. Shinohara, Astrophys. J. **714**, 915 (2010).
[32]F. Guo, H. Li, W. Daughton, and Y. Liu, Phys. Res. Lett. **113**, 155005 (2014).
[33]J. F. Drake, M. Swisdak, K. M. Schoeffler, B. N. Rogers, and S. Kobayashi, Geophys. Res. Lett. **33**, L13105, doi:10.1029/2006GL025957 (2006).
[34]R. Wang, Q. Lu, X. Li, C. Huang, and S. Wang, J. Geophys. Res. **115**, A11201, doi:10.1029/2010JA015473 (2010).
[35]C. Huang, Q. Lu, Z. Yang, M. Wu, Q. Dong, and S. Wang, Nonlinear Processes Geophys. **18**, 727 (2011).
[36]K. G. Tanaka, M. Fujimoto, S. V. Badman, and I. Shinohara, Phys. Plasmas **18**, 022903 (2011).
[37]A. Le, H. Karimabadi, J. Egedal, V. Roytershteyn, and W. Daughton, Phys. Plasmas **19**, 072120 (2012).
[38]M. Zhou, Y. Pang, X. Deng, S. Huang, and X. Lai, J. Geophys. Res. **119**, 6177, doi:10.1002/2013JA019483 (2014).
[39]H. Wang, Q. Lu, C. Huang, and S. Wang, Astrophys. J. **821**, 84 (2016).
[40]R. Wang, Q. Lu, R. Nakamura, C. Huang, A. Du, F. Guo, W. Teh, M. Wu, S. Lu, and S. Wang, Nat. Phys. **12**, 263 (2015).
[41]Y. Zhao, R. Wang, Q. Lu, A. Du, Z. Yao, and M. Wu, J. Geophys. Res. **121**, 10898, doi:10.1002/2016JA023526 (2016).
[42]T. Northrop, *The Adiabatic Motion of Charged Particles* (John Wiley and Sons, New York, 1963).
[43]J. T. Dahlin, J. F. Drake, and M. Swisdak, Phys. Plasmas **21**, 092304 (2014).
[44]N. Aunai, M. Hesse, and M. Kuznetsova, PhPl **20**, 092903 (2013).
[45]W. Daughton, V. Roytershteyn, H. Karimabadi, L. Yin, B. J. Albright, B. Bergen, and K. J. Bowers, Nat. Phys. **7**, 539 (2011).
[46]L. S. Shepherd and P. A. Cassak, Phys. Rev. Lett. **105**, 015004 (2010).